Materials Science and Engineering, Volume 45, No. 1 (2020), pp. 163–170.
DOI: 10.32974.mse.2020.016

SYNTHESIS AND CHARACTERIZATION OF MAGNETIC NANOPARTICLES FOR BIOLOGICAL SEPARATION METHODS

ÁGNES MÁRIA ILOSVAI[1] – EMMA SZŐRI-DOROGHÁZI[2] –
ÁDÁM PREKOB[3] – LÁSZLÓ VANYOREK[4]

Abstract: In our work, we successfully combined sonochemical production with the combustion method to produce magnetic nanoparticles. Iron (II)-acetate and iron (III)-citrate precursors were used in the synthesis, which in both cases were dispersed in 400 g/mol polyethylene glycol (PEG 400) using a high-efficiency ultrasonic technique (Hielscher homogenizer). The magnetic nanoparticles were bound to DNA to test their applicability in DNA separation processes. Plasmid DNA from *Escherichia coli (E. coli)* is well suited for carrying out the above assays. The magnetic particle morphology and size distribution were investigated by transmission electron microscopy (TEM), the nanoparticles were characterized by a high degree of dispersion. The functional groups on the surface of the particles were identified by Fourier transform infrared spectroscopy (FTIR) and hydroxyl groups were detected. The iron oxide forms of the sample were identified with X-ray diffraction (XRD), which were magnetite, maghemite and hematite phases. The dispersibility of nanoparticles in aqueous media was characterized by measuring the electrokinetic potential (using DLS) of the particles and due to the hydroxyl groups, its surface was sufficiently dispersible.

Keywords: nanoparticles, magnetite, TEM, FTIR, XRD, DNA

INTRODUCTION

In this research, we prepared and characterized magnetic iron oxide nanoparticles. Our goal was to produce nanoparticles that can be well dispersed in aqueous medium forming a stable dispersion. Due to their favorable properties, they are suitable for biological applications like DNA binding assays. At the moment, the commercially available DNA separation kits operating on a similar principle are available at high prices (Anti-DYKDDDDK antibody magnetite, of which 10 ml: approximately HUF 570,000) [1].

[1] Institute of Chemistry, University of Miskolc
H-3515 Miskolc-Egyetemváros, Hungary
ilosvaiagnes001@gmail.com
[2] Institute of Chemistry, University of Miskolc
H-3515 Miskolc-Egyetemváros, Hungary
emma.szdoroghazi@uni-miskolc.hu
[3] Institute of Chemistry, University of Miskolc
H-3515 Miskolc-Egyetemváros, Hungary
prekob.a@gmail.com
[4] Institute of Chemistry, University of Miskolc
H-3515 Miskolc-Egyetemváros, Hungary
vanyorekl@gmail.com

Many production processes are already known according to literature like sol-gel technology, microemulsion process, hydrothermal synthesis, high-temperature decomposition, precipitation synthesis, and sonochemical (ultrasonic) process [2]. Magnetic nanoparticles are used in many fields, including the pharmaceutical, food, and electronics industries, but we also find examples of their biological, geochemical, chemical, and electronic applications [2, 3].

Magnetic fluids and aqueous nanoparticles, which are particularly useful in biological and medical diagnostic applications, have been used as contrast agents in MRI (magnetic resonance imaging) studies. Magnetic particles have also been successfully tested in targeted transport of active substances during hyperthermia, and in magnetic cell separation processes [4–11]. Particles with different (polymer) coatings are widely used in DNA purification [12–15]. Most magnetic materials used for DNA purification have a complex composition, making them expensive to produce. Our choice of topic was influenced by the high price of the used commercial materials so we tried and successfully prepared magnetic iron oxide nanoparticles with properties similar to commercially available magnetites with a cheaper production process.

1. MATERIALS AND METHODS

For the production of magnetite nanoparticles iron (II) acetate, $Fe(CO_2CH_3)_2$ (Aldrich Chemistry) and iron (III) citrate, $FeC_6H_5O_7 \cdot xH_2O$ (PanReac AppliChem) salts were used, in both cases dispersed in polyethylene glycol with a molecular weight of 400 g/mol, $HO(C_2H_4O)_nH$ (Merck). For the synthesis, we used a high-efficiency ultrasonic homogenizer, Hielscher UIP1000hdT. The morphological characterization of the particles was performed by transmission electron microscopy (TEM; FEI Technai G), the functional groups were identified by Fourier transform infrared spectroscopy (FTIR; Bruker Vertex 70 FTIR spectroscope). The phase composition was determined by X-ray diffraction measurement (XRD; Rigaku Miniflex). To measure the electrokinetic potential of the particles, dynamic light scattering (DLS; Malvern, Zetasizer Nano-ZS) was used. The carbon content of the samples was determined with a CHNS (Vario MACRO) analyzer. The efficiency of DNA binding assays was confirmed by gel electrophoresis.

2. PRODUCTION OF MAGNETIC NANOPARTICLES AND DNA BINDING ASSAY

In this work, we would like to present magnetic nanoparticles from two different precursors: **sample A1** [iron (II) acetate] and **sample D1** [iron (III) citrate].

Both samples were prepared the same way, only the precursor type was changed. During the synthesis, 2 g of the precursor was used for **sample A1** (for **sample D1**: 3.47 g), which was dispersed in 20 g of polyethylene glycol (PEG) with a molecular weight of 400 g/mol using a high-efficiency ultrasonic homogenizer (Hielscher UIP1000hdT). After finishing the sonochemical treatment, the polyethylene glycol was burned using a Bunsen burner, thus creating iron oxide samples with magnetic

properties. Since **sample A1** was stable in aqueous medium, only the **D1 sample** had to be stabilized. For this purpose 5 different stabilizers were used: *PVP K30* (Polyvinylpyrrolidone); *PVA 115000* (polyvinyl alcohol); *CMC* (carboxymethylcellulose); *PEG 1000* (polyethylene glycol 1000) and *clay mineral* (sodium bentonite).

During the DNA binding examinations of the samples, the first step was mixing the DNA and the magnetic nanoparticles (MNPs) in a certain ratio (**sample A1**: 2 mg/ml; **sample D1**: around 2 mg/ml and 20 mg/ml). After the bonding of the DNA on the MNPs surfaces, they were collected at the bottom of the tube using a strong magnet. The supernatant fraction was also sampled, followed by washing of the samples. This is followed by the separation of DNA molecules from particles. Finally, the DNA eluted from the surface of the particles was placed in a separated sample holder *(Figure 1)*.

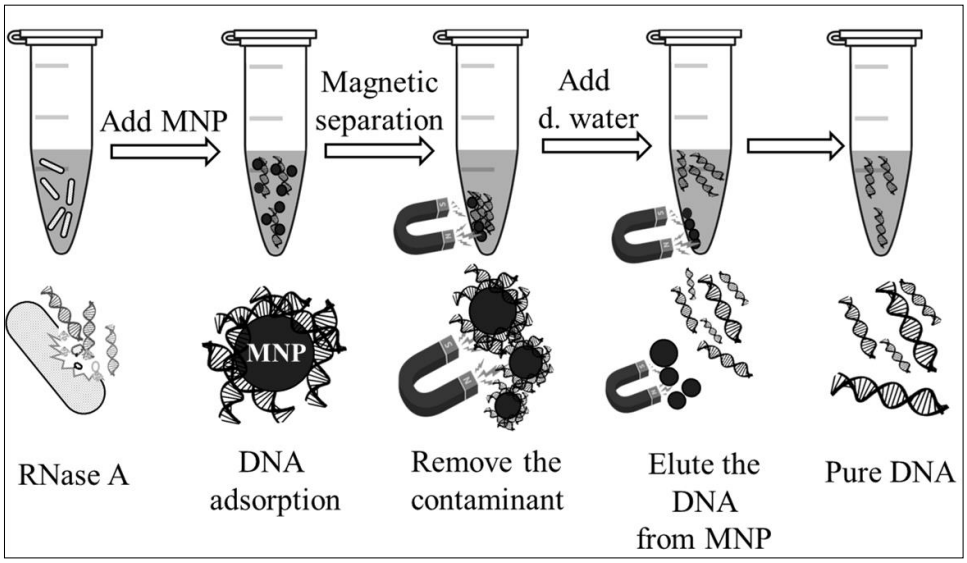

Figure 1
Outline of DNA binding test

3. EXPERIMENTAL RESULTS AND THEIR EVALUATION

The samples were first examined by transmission electron microscopy, with which the particle size and the morphology of the particles were characterized.

The granular structure can be well observed in the TEM images of both **sample A1** and **D1** *(Figure 2)*, so in both cases, we made size distribution diagrams using the "ImageJ" software *(Figure 3/A, B)*. The diagrams show that the average particle size of **sample A1** *(Figure 3/A)* was 14.4 nm, while the average particle size of **sample D1** *(Figure 3/B)* was 23.9 nm.

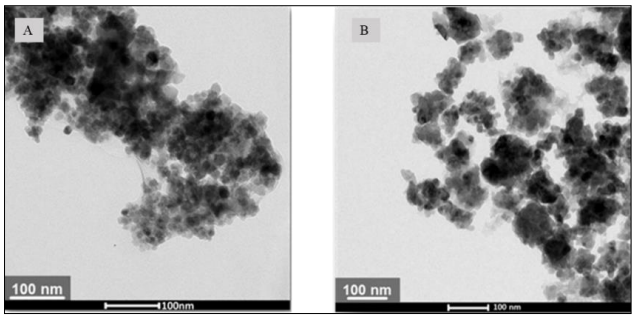

Figure 2
*TEM recording of **sample A1** and **D1***

Using Fourier transform infrared spectroscopy (FTIR), the functional groups on the surface of the particles were identified *(Figure 3/C, D)*. Comparing the spectra, it can be said that in both cases the valence vibrations of the Fe-O and OH groups can be found, C = C valence vibrations can also be seen in the mentioned samples, and C-O bonds can also be identified. Asymmetric and symmetric CH bonds can also be observed for **sample D1**.

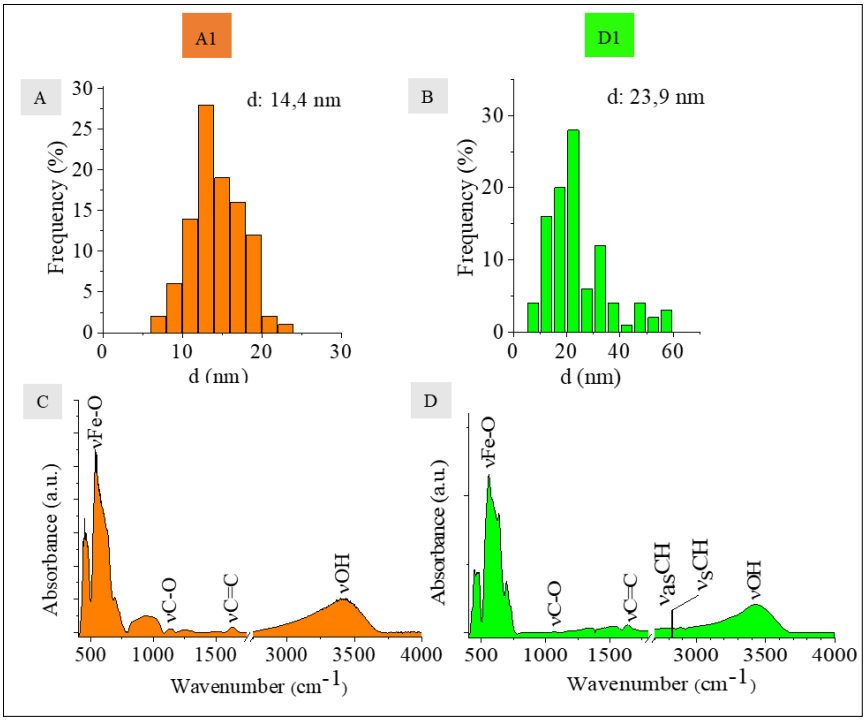

Figure 3
Size distribution diagrams (A, B) and FTIR spectra (C, D)

CHNS elemental analysis was performed on the samples to find out the exact amount of carbon because this may affect the ability of the particles to bind DNA. Elemental analysis showed that the carbon content in **sample A1** was 5.1 w/w%, while in **sample D1** this ratio was more than twice, 10.75 w/w% by number.

The phase composition of the samples was determined by X-ray diffraction (XRD) measurement. In case of sample A1 the results revealed *(Figure 4/A)* that there were three different iron oxide phases in the sample: magnetite (Fe_3O_4), hematite (α-Fe_2O_3) and maghemite (γ-Fe_2O_3). The sample contained 61.8 w/w% maghemite, the magnetite content was 19.9 w/w%, and the amount of hematite was 18.3 w/w%. In case of the **sample D1** *(Figure 4/B)* only two phases were detected, 93.2 w/w% maghemite and 6.8 w/w% hematite. In the case of **sample D1**, the ratio of the non-magnetic phase (hematite) was reduced (6.8 w/w%).

Based on the DLS results *(Figure 4/C)*, the deprotonation of the hydroxyl groups on the surface of the magnetic nanoparticles resulted in a negative zeta potential with an average of –20.3 mV. By reducing the zeta potential, the stability of aqueous dispersions made of nanoparticles can be increased.

The zeta potential of **sample D1** was also measured *(Figure 4/D)*, which showed an average of –4.1 mV, which is less negative than the determined potential for **sample A1** (–20.3 mV).

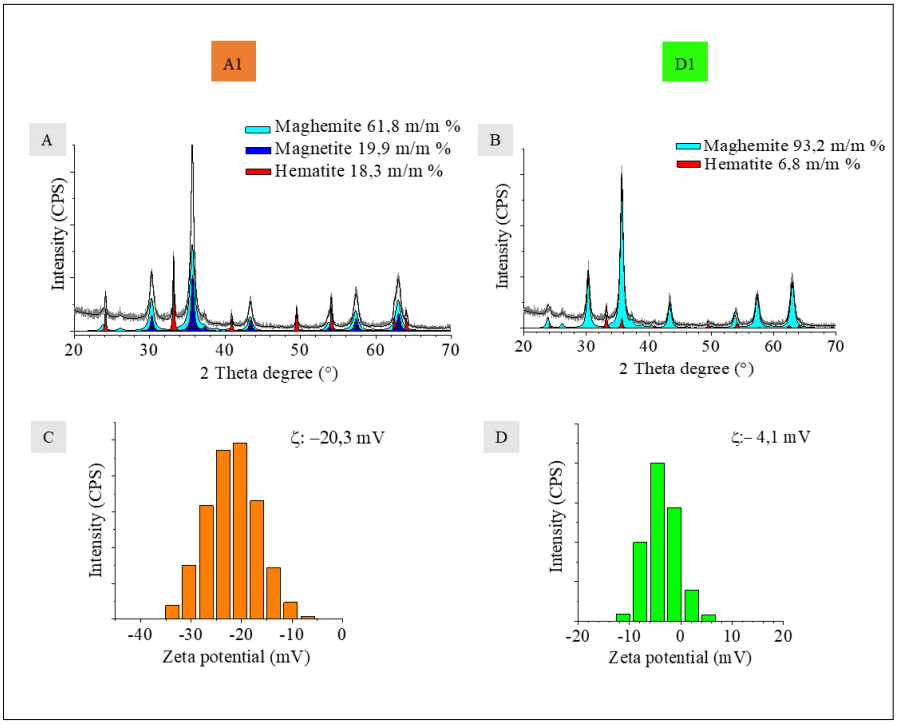

Figure 4

X-ray diffractograms (A, B) and Zeta potential distribution diagrams (C, D)

Both samples were tested in DNA binding assays. For **sample A1** *(Figure 5)*, the order of the samples in the gel electrophoresis assays was as follows:

Column 1: Positive control (+): plasmid DNA purified from *E. coli*

Column 2: MW marker (molecular weight marker): 1 kb DNA molecular weight marker

Column 3: Sample from supernatant fraction

Column 4, 6, 8: Negative control (–)

Column 5: DNA sample recovered from the MNP (eluted) (EF = elution fraction)

Column 7: Sample taken from the second elution of the DNA-MNP mixture (eluted DNA)

The test results showed that in the case of **sample A1**, the DNA bonds well to the surface of the particles and can be eluted from there *(Figure 5/A1)*. The DNA was able to bind reversibly because the red fluorescent band indicating the presence of DNA detached from the surface of the particles (lane 5 on the gel plate) is visible.

For *Figure 5/D1* the positive control (+) is the first column, which also contains plasmid DNA from *E. coli*. Next to it is the MW marker, which is a 1 kb DNA molecular weight marker, 3–4. columns denote the F1 fraction, the 5–6. columns are the supernatant fraction of DNA samples. The 7–8. column shows EF (column 7: about 2 mg/ml sample D1 + DNA sample; column 8: about 20 mg/ml sample D1 + DNA sample), which is the fraction taken from the DNA fraction separated from the DNA-MNP system.

For **sample D1** *(Figure 5/D1)*, only a faint mark is seen in EF (columns 7–8), suggesting that the DNA-binding ability of **sample D1** worked very well and we could not use this elution method, which was used for **sample A1**. In the further research more tests will be executed with this sample using new eluents.

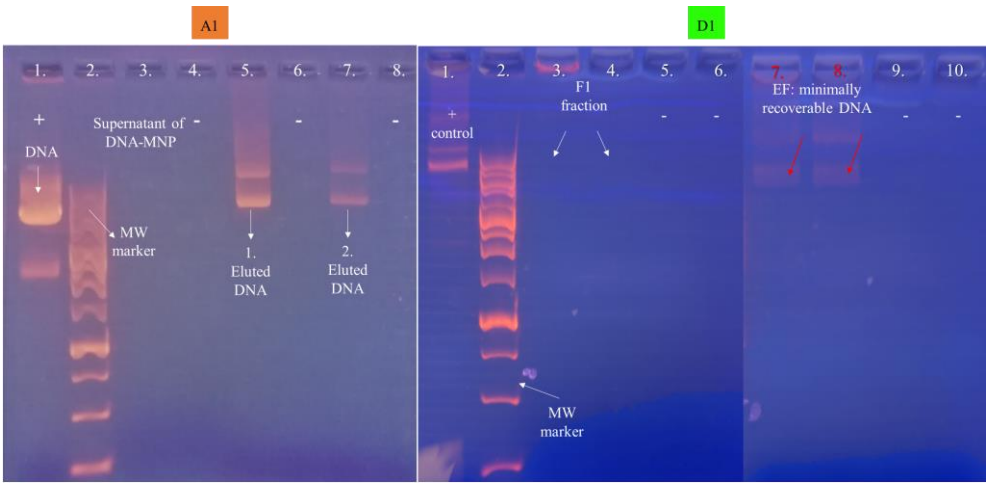

Figure 5
Investigation of reversible DNA binding by gel electrophoresis on samples A1 and D1

CONCLUSION

Magnetic nanoparticles were prepared using different iron precursors (**sample A1**: iron (II) acetate, **sample D1**: iron (III) citrate) and characterized by XRD, TEM, DLS and FTIR methods. The synthesis of magnetic iron oxides was accomplished by combining two modern methods, the sonochemical and the combustion methods. A recipe (**sample A1**) was also created with which we could produce a material suitable for DNA purification, which is more economical to prepare than the others available on the market.

ACKNOWLEDGEMENTS

The described article/presentation/study was carried out as part of the EFOP-3.6.1-16-2016-00011 *Younger and Renewing University – Innovative Knowledge City – institutional development of the University of Miskolc aiming at intelligent specialisation* project implemented in the framework of the Szechenyi 2020 program. The realization of this project is supported by the European Union, co-financed by the European Social Fund.

REFERENCES

[1] Anti-DYKDDDDK tag Affinity Beads (Binds to FLAG® tag sequence), Abcam. Available: https://www.abcam.com/ (2020. 04. 29.).

[2] Tóth, I. (2013). *Synthesis of variable-sized magnetite nanoparticles and their surface modification by polianionic coatings*. Dissertation (Doctoral dissertation), University of Szeged.

[3] Szebeni, J. (2011). Nanomedicine: Application of Nanotechnology in Medicine. Opportunities in Neuropsychiatry. Nanomedicine Research and Training Center, Semmelweis University, Bay Zoltán Public Foundation for Applied Research, Budapest, Uni. Miskolc, Faculty of Health, Miskolc, *Neuropsychopharmacologia Hungarica*, Vol. XIII, No 1, p. 17.

[4] McKeehan, L. W. (1940). Optical and Magnetic Properties of Magnetite Suspensions, Surface Magnetization in Ferromagnetic Crystals. *Phys. Rev*., Vol. 57, No. 12, pp. 1177–1178., June 15, 1940.

[5] Bee, A., Massart, R., Neveu, S. (1995). Synthesis of very fine maghemite particles. *Journal of Magnetism and Magnetic Materials*, Vol. 149, pp. 6–9.

[6] Blanco-Mantecon, M., O'Grady, K. (2006). Interaction and size effects in magnetic nanoparticles. *Journal of Magnetism and Magnetic Materials*, Vol. 296, pp. 124–133., Jan 2006.

[7] Fauconnier, N., Bée, A., Roger, J., Pons, J. N. (1999). Synthesis of aqueous magnetic liquids by surface complexation of maghemite nanoparticles. *Journal of Molecular Liquids*, Vol. 83, pp. 233–242., Dec 1999.

[8] Pankhurst, Q. A., Connolly, J. S., Jones, S. K., Dobson, J. (2003). Applications of magnetic nanoparticles in biomedicine. *Journal of Physics; Applied Physics*, Vol. 36, pp. R167–R181., July 2003.

[9] Gupta, A. K., Gupta, M. (2005). Synthesis and surface engineering of iron oxide nanoparticles for biomedical applications. *Biomaterials*, Vol. 26, No. 18, pp. 3995–4021., June 2005.

[10] Jain, T. K., Richey, J., Strand, M., Leslie-Pelecky, D. L., Flask, C. A., Labhasetwar, V. (2008). Magnetic nanoparticles with dual functional properties: Drug delivery and magnetic resonance imaging. *Biomaterials*, Vol. 29, No 29. pp. 4012–4021., Oct. 2008.

[11] Munnier, E., Cohen-Jonathan, S., Linassier, C., Douziech-Eyrolles, L., Marchais, H., Soucé, M., Hervé, K., Dubois, P., Chourpa, I. (2008). Novel method of doxorubicin–SPION reversible association for magnetic drug targeting. *International Journal of Pharmaceutics*, Vol. 363, No. 1–2, pp. 170–176., 3 Nov 2008.

[12] Saiyed, Z. M., Bochiwal, C., Gorasia, H., Telang, S. D., Ramchand, C. N. (2006). *Application of magnetic particles (Fe_3O_4) for isolation of genomic DNA from mammalian cells*. Department of Biochemistry, Faculty of Science, Maharaja Sayajirao University of Baroda, Sayajigunj, 7 July 2006.

[13] Yuanling, S., Jianbo, L., Yanhui, W., Chaofan, D., Yanna, L., Weiyan, S., Chuannan, L. (2017). A chemiluminescence biosensor based on the adsorption recognition function between Fe_3O_4@SiO_2@GO polymers and DNA for ultrasensitive detection of DNA. *Spectrochimica Acta Part A: Molecular and Biomolecular Spectroscopy*, University of Jinan, China, Vol. 178, pp. 1–7.

[14] Rahnama, H., Sattarzadeh, A., Kazemi, F., Ahmadi, N., Sanjarian, F., Zand, Z. (2016). Comparative study of three magnetic nano-particles ($FeSO_4$, $FeSO_4/SiO_2$, $FeSO4/SiO_2/TiO_2$) in plasmid DNA extraction. *Analytical Biochemistry*, Vol. 513, pp. 68–76.

[15] Nahid, S., Alireza, A., Mina, J., Monireh, F. (2016). Functionalization of Fe_3O_4@SiO_2 magnetic nanoparticles with nicotinamide and in-vitro DNA interaction. *Journal of Molecular Liquids*, Vol. 224, pp. 227–233.